Healthcare Analytics 4 (2023) 100275

Contents lists available at ScienceDirect

Healthcare Analytics

journal homepage: www.elsevier.com/locate/health

# A deterministic compartmental model for investigating the impact of escapees on the transmission dynamics of COVID-19

Josiah Mushanyu [a,b], Chidozie Williams Chukwu [c,*], Chinwendu Emilian Madubueze [d,e], Zviiteyi Chazuka [f], Chisara Peace Ogbogbo [g]

[a] Department of Computing, Mathematical, and Statistical Sciences, University of Namibia, Windhoek 13301, Windhoek, Namibia
[b] Department of Mathematics and Computational Sciences, University of Zimbabwe, Box MP 167 Mount Pleasant, Harare, Zimbabwe
[c] Department of Mathematics, Wake Forest University, Winston-Salem, NC 27109, USA
[d] Department of Mathematics, Joseph Sarwuan Tarkaa University Makurdi, Nigeria
[e] Department of Mathematics and Statistics, York University, Toronto, Canada
[f] Department of Decision Sciences, College of Economics and Management Sciences, University of South Africa, South Africa
[g] Department of Mathematics, University of Ghana, Ghana

ARTICLE INFO

*Keywords:*
Deterministic model
Correlation
COVID-19
Numerical simulations
Quarantine
Escapees

ABSTRACT

The recent outbreak of the novel coronavirus (COVID-19) pandemic has devastated many parts of the globe. Non-pharmaceutical interventions are the widely available measures to combat and control the COVID-19 pandemic. There is great concern over the rampant unaccounted cases of individuals skipping the border during this critical period in time. We develop a deterministic compartmental model to investigate the impact of escapees (individuals who evade mandatory quarantine) on the transmission dynamics of COVID-19. A suitable Lyapunov function has shown that the disease-free equilibrium is globally asymptotically stable, provided $\mathcal{R}_0 < 1$. We performed a global sensitivity analysis using the Latin-hyper cube sampling method and partial rank correlation coefficients to determine the most influential model parameters on the short and long-term dynamics of the pandemic to minimize uncertainties associated with our variables and parameters. Results confirm a positive correlation between the number of escapees and the reported COVID-19 cases. It is shown that escapees are primarily responsible for the rapid increase in local transmissions. Also, the results from sensitivity analysis show that an increase in governmental role actions and a reduction in the illegal immigration rate will help to control and contain the disease spread.

## 1. Introduction

The novel Coronavirus (COVID-19), which has taken the world by surprise since its first case in Wuhan, China, in December 2019, has ravaged Africa, and Zimbabwe has felt its negative impact. As of the 14th of July 2020, there were 13,141,440 confirmed cases worldwide and 573,349 deaths. The United States of America was the most affected country in the world, with 3,481,677 confirmed COVID-19 infections and 138,291 deaths [1]. In Africa, South Africa is currently the epicenter of the coronavirus, with 287,796 confirmed cases and 4172 deaths [2]. Zimbabwe recorded its first COVID-19 case on the 20th of March 2020 and its first death was recorded on the 23rd of March 2020 [3]. Thereafter, the government of Zimbabwe imposed a 21-day nationwide lockdown on the 30th of March 2020 [3]. When this manuscript was drafted, Zimbabwe recorded 1034 confirmed cases with 19 deaths [3].

Recently, Zimbabwe experienced a sharp spike in the number of confirmed COVID-19 cases despite the lockdown. The sharp spike was suspected to be due to the increase in the number of returnees from other countries. As a measure to control the spread of the infection, Zimbabwe closed her borders to normal traffic except that of returnees and essential services. Also, the government imposed a mandatory 21-day quarantine on all returnees, a measure that helped identify quarantined returnees who tested positive early. These were immediately placed under mandatory isolation within the country's isolation healthcare centers. However, some of the returnees escaped from the quarantine centers either after they had tested positive or simply because they did not want to stay at the quarantine centers. This led to escapees exposing individuals in the community to COVID-19. Escapees in this study refer to those individuals who decided to evade the mandatory quarantine on all returnees (Zimbabwean citizens

* Corresponding author.
*E-mail address:* wiliam.chukwu@gmail.com (C.W. Chukwu).

https://doi.org/10.1016/j.health.2023.100275
Received 28 May 2023; Received in revised form 29 September 2023; Accepted 21 October 2023
Available online 31 October 2023

who had moved out of the country for various reasons such as work, business, or tourism, and other foreign nationals who were visiting the country) upon being frustrated by the length of stay in quarantine imposed by the Zimbabwean government. We use escapees in this context to refer to this act of evading a mandatory and monitored quarantine as reported in private and government-owned media. As of 10 July 2020, there were 209 escapees from quarantine centers; the police arrested only 28 of them, leaving 181 escapees unaccounted for [4]. Among these escapees, it was also reported that some had tested positive, implying that there was a high possibility of spreading the infection.

The global economic impact of the novel COVID-19 has brought researchers from across the globe together to fight the virus through various research works. These works include the mathematical modeling of the impact of COVID-19 within countries such as South Africa, China, the United States and India, to name a few [5–17], control strategies [18–20] and the impact assessment of the control strategies and their sensitivity [21–25] on COVID-19. Most of the mathematical models developed used an $SEIR$ modeling framework, which only varied in the descriptions of the compartments used and the results obtained from the studies. The main thrust of the mathematical modeling approaches was to predict the future trend of the COVID-19 virus and provide recommendations to policymakers on the way forward. The role of governmental action in controlling the spread of COVID-19 within communities was modeled by Mushayabasa et al. [5]. In their work, they presented a model that looked at the effects of actions such as imposed social distancing measures, travel restrictions, quarantine, sanitizing and hospitalization on the control of the transmission dynamics of COVID-19. Results from the study indicated that intervention methods by the government positively impact the reduction of infection, and the authors also suggested important thresholds by which these intervention strategies must be bound. Nyabadza et al. [26] also modeled the effect of one governmental action (social distancing) on the South African population. Results of their study indicated that if social distancing is relaxed by as much as 2%, it could have an impact of 23% rise in infections while an increase in social distance adherence by 2% could effectively reduce infections by 18% [26]. Ambikapathy et al. [27] assessed the effect of the imposed lockdown on the transmission dynamics of COVID-19 in India, and results from the model suggested that a 21-day lockdown was effective in the reduction of infections in India and if the government could increase lockdown to 42 days the infections would further be reduced. Other mathematical models of note on the subject matter include [28–31], just to mention a few.

The model developed in this paper was designed to study the contribution of escapees on local COVID-19 transmissions during the period of imposition of mandatory lockdown in Zimbabwe. This model gives a first attempt to investigate escapees' contribution to COVID-19 disease spread. The model is applied to data on COVID-19 cases in Zimbabwe during the period of mandatory lockdown and returnee quarantine. It is essential to quantify the contribution of escapees to local transmissions and assess the implications for public health and policy-making. Thus, we focus on the effects of quarantine measures on the dynamics of COVID-19 infection within the Zimbabwean population. Of particular note, the paper looks at the effects of those who escape from quarantine facilities on the dynamics of COVID-19 in Zimbabwe. We employ advanced mathematical and statistical techniques, such as the global sensitivity analysis using the Latin-hypercube sampling method and partial rank correlation coefficients. These techniques allow the identification of the most influential model parameters responsible for driving both short and long-term COVID-19 pandemic dynamics. By reducing uncertainties surrounding influential variables and parameters, the results of this study will provide more accurate and actionable recommendations for policymakers and public health officials. These results can also be applied in other countries across the globe with similar challenges in quarantining individuals.

The next section, Section 2, presents the model formulation, while Section 3 presents the model analysis. Numerical simulations and global uncertainty analysis are carried out in Section 4. The paper is concluded in Section 5.

## 2. Model formulation

The human population is subdivided into 8 distinct classes namely; the susceptible individuals, $S(t)$, returnees in quarantine who were not exposed to COVID-19, $Q_1(t)$, returnees in quarantine who were exposed to COVID-19, $Q_2(t)$, locals who are exposed to COVID-19, $E(t)$, undetected infected individuals, $I(t)$, detected and isolated individuals, $I_D(t)$, recovered individuals, $R(t)$ and deceased individuals, $D(t)$. We assume that the population mixes homogeneously. The returnees coming into the country are classified as $Q_1(t)$ and $Q_2(t)$, where $Q_1(t)$ denotes returnees who undergo quarantine within the country's centers as prescribed by the government but are found to be COVID-19 negative after completing quarantine. Upon completion of quarantine, these individuals are assumed to enter class $S(t)$ at a rate, $\theta$, as they remain susceptible to local infections. The recruitment rate of returnees is given by $\Lambda$. A proportion, $\Pi$, join the class $Q_1(t)$ and the remainder $(1-\Pi)$ join the class $Q_2(t)$. The model assumes that a proportion, $q\phi$, of individuals in $Q_2(t)$ will escape quarantine while positive and hence join class $I(t)$ of undetected infected individuals, where $q$ is the probability of escape and $\phi$ is the escape rate. The remaining proportion $(1-q)\phi$ from $Q_2(t)$ undergo testing and may be found positive and proceed to join class $I_D(t)$. The rationale here is that returnees are tested at the beginning of quarantine, during quarantine, and towards the end of quarantine. During these prescribed periods, an individual may be found positive and proceed to class $I_D(t)$ or escape while positive, avoiding further probation. It is assumed that the exposed individuals who are locals, $E(t)$, become undetected infected individuals at a rate, $\sigma$ because they are yet to be detected via testing while individuals infected with COVID-19 in class $I(t)$ are detected through testing at a rate, $\delta_1$ and isolated. Since the beginning of the outbreak, scientists have suggested the possible mutation of the severe acute respiratory syndrome coronavirus 2 (SARS-Cov-2) virus [32]. According to their research, these mutations may cause the weakening of the strength of the virus. At the same time, some individuals may develop resistance and can fight off the virus without seeking medical attention. We thus assume that the recovery of undetected infected individuals, $I(t)$, occurs at a rate, $\delta_2$ and moves to class $R(t)$. However, a certain proportion of infected individuals will succumb to the infection at a rate $\delta_3$ and move into class $D(t)$, which is the death class. A proportion, $d$, of individuals that have been detected (and isolated) in $I_D(t)$ recover at a rate $\rho$ and join class $R(t)$ of recovered individuals. The remaining proportion $(1-d)\rho$ succumb to the infection and join class $D(t)$. We assume permanent immunity of recovered individuals since the model only considers a short period covering lockdowns. The model has two infectious compartments, $I(t)$ and $I_D(t)$. Hence, we assume that the force of infection for the model is given by

$$\lambda = \frac{\beta(1-\kappa)\left(I+\eta I_D\right)}{N}, \tag{1}$$

where $\beta$ is the transmission rate of COVID-19, $\eta$ is the modification parameter, where $0 \leq \eta \leq 1$ and the term $(1-\kappa)$ represents the effects of governmental action such as wearing of face masks, sanitization, social distancing etc., where $0 \leq \kappa \leq 1$. A value of $\kappa$ close to 1 indicates that governmental action is effective while a value of $\kappa$ close to zero implies that there is little or no governmental action. The model does not include the vital dynamics. The population total is given by

$$N = S(t) + E(t) + Q_1(t) + Q_2(t) + I(t) + I_D(t) + R(t) + D(t).$$

The model dynamics can be summarized as in Fig. 1.

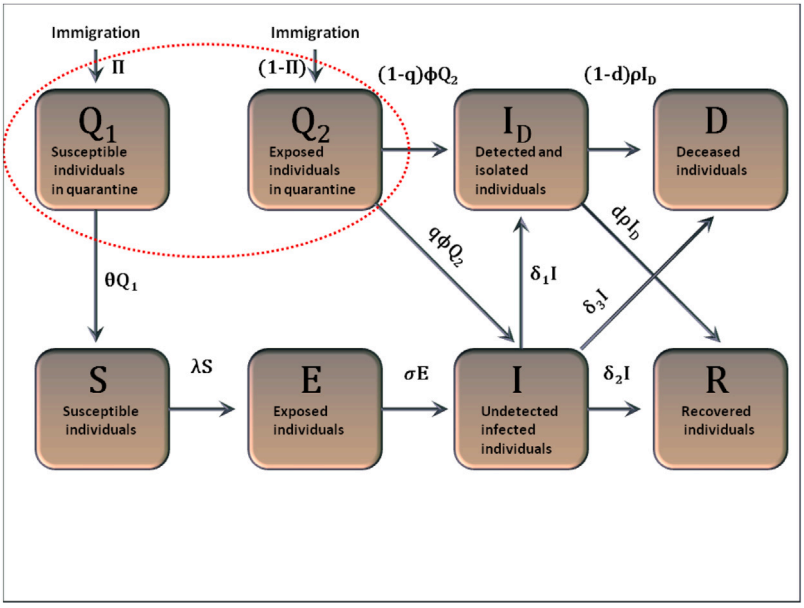


**Fig. 1.** Model flow diagram. The dotted red oval indicates quarantined individuals.

The description of model variables, parameters and assumptions combined with the model flow diagram (Fig. 1) leads to the following set of non-linear ordinary differential equations:

$$\left.\begin{aligned} S' &= \theta Q_1 - \lambda S, \\ E' &= \lambda S - \sigma E, \\ I' &= \sigma E + q\phi Q_2 - (\delta_1 + \delta_2 + \delta_3) I, \\ I_D' &= (1-q)\phi Q_2 + \delta_1 I - \rho I_D, \\ Q_1' &= \Pi \Lambda - \theta Q_1, \\ Q_2' &= (1-\Pi)\Lambda - \phi Q_2, \\ R' &= \delta_2 I + d\rho I_D, \\ D' &= \delta_3 I + (1-d)\rho I_D, \end{aligned}\right\} \tag{2}$$

with the initial conditions

$$S(0) > 0, E(0) \geq 0, I(0) \geq 0, I_D(0) \geq 0, Q_1(0) > 0, Q_2(0) \geq 0, R(0) \geq 0 \text{ and } D(0) \geq 0.$$

Here, all the model parameters are considered to be non-negative.

Fig. 1 correctly captures the epidemiological status of the returnees. However, for simplicity, we assume that all uninfected quarantined individuals will eventually join the class $S(t)$ of susceptible, as shown in Fig. 1. This basically means incorporating some people who are in quarantine in the susceptible population. The error that results from this consideration is negligible. Further, we assume that all the remaining quarantined individuals will either escape to join the class $I(t)$ or move to the class of detected and isolated individuals upon being screened through testing, which is a similar modification done for (SARS-Cov-2) model by Gumel et al. [33]. This is related to this work regarding a respiratory disease like COVID-19. They also considered the impact of undetected entry of infected individuals on the SARS transmission dynamics. Thus, the modified model can be represented by Fig. 2.

We have the following set of nonlinear ordinary differential equations for the modified model:

$$\left.\begin{aligned} S' &= -\lambda S, \\ E' &= \lambda S - \sigma E, \\ I' &= \sigma E + q\phi Q_2 - (\delta_1 + \delta_2 + \delta_3) I, \\ I_D' &= (1-q)\phi Q_2 + \delta_1 I - \rho I_D, \\ Q_2' &= \Lambda - \phi Q_2, \\ R' &= \delta_2 I + d\rho I_D, \\ D' &= \delta_3 I + (1-d)\rho I_D, \end{aligned}\right\} \tag{3}$$

with the initial conditions

$$S(0) > 0, E(0) \geq 0, I(0) \geq 0, I_D(0) \geq 0, Q_2(0) \geq 0, R(0) \geq 0 \text{ and } D(0) \geq 0,$$

where all the model parameters are considered to be non-negative. Here, $\Lambda$ is the recruitment rate of COVID-19-exposed individuals returning to the country.

## 3. Model analysis

### 3.1. Positivity of solutions

We now consider the positivity of system (3). We show that all the state variables remain non-negative, and the solutions of system (3) with positive initial conditions remain positive for all $t > 0$.

**Theorem 1.** *Given that the initial conditions of system (3) are* $S(0) > 0, E(0) \geq 0, I(0) \geq 0, I_D(0) \geq 0, Q_2(0) \geq 0, R(0) \geq 0$ *and* $D(0) \geq 0$, *then for all* $t > 0$, *all solutions of model system (3) remain positive in* $\mathbb{R}^7_+$.

**Proof.** Following the approach in Gweryina et al. [34], we assume that

$$t_1 = sup\left\{t > 0 : S(0) > 0, E(0) \geq 0, I(0) \geq 0, I_D(0) \geq 0, Q_2(0) \geq 0, R(0) \geq 0, D(0) \geq 0 \in [0, t]\right\}.$$

Thus, $t_1 > 0$ and it follows from the first equation of system (3) that

$$\frac{dS}{dt} = -\lambda S. \tag{4}$$

Solving this using separation of variables yields

$$\ln S = -\int_0^{t_1} \lambda(t)dt + K. \tag{5}$$

Hence,

$$S(t) \geq A \exp\left[-\int_0^{t_1} \lambda(t)dt\right], \tag{6}$$

where $A$ is a constant to be determined. Therefore, applying initial conditions $S(0) = S_0$ yields $A = S_0$ such that

$$S(t) \geq S_0 \exp\left[-\int_0^{t_1} \lambda(t)dt\right] > 0. \tag{7}$$

Therefore, it can be shown in a similar manner that $E(t) \geq 0, I(t) \geq 0, I_D(t) \geq 0, Q_2(t) \geq 0, R(t) \geq 0$ and $D(t) \geq 0$, for all $t > 0$. This concludes the proof. □

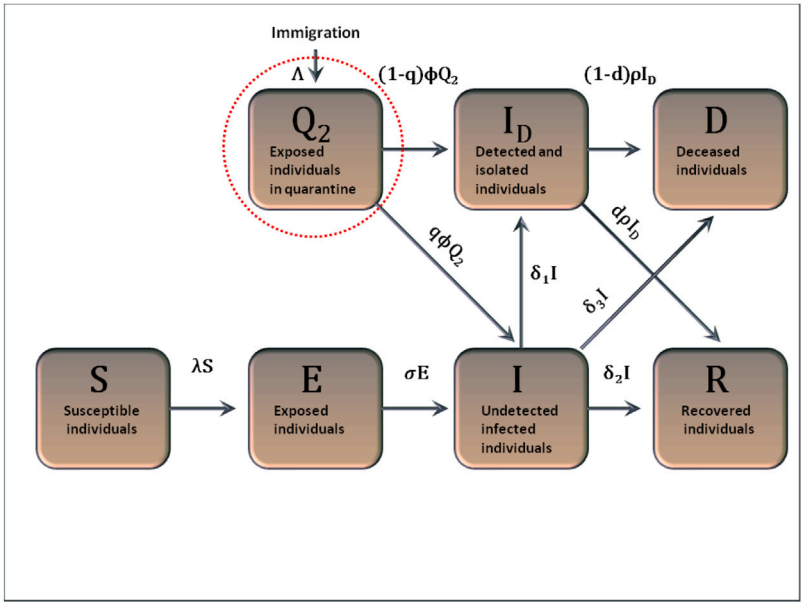


**Fig. 2.** Model flow diagram. The dotted red oval indicates quarantined individuals.

### 3.2. Invariant region

**Theorem 2.** *The region*

$$\Omega = \left\{(S, E, I, I_D, Q_2, R, D) \in \mathbb{R}_+^7 : S(t) + E(t) + I(t) + I_D(t) + Q_2(t) + R(t) + D(t) \leq N_0\right\}$$

*is positively invariant for system (3), with non-negative initial conditions where $N_0$ is the initial population.*

**Proof.** Adding all the equations of system (3) yields

$$\frac{dN}{dt} = 0.$$

Then, $\limsup_{t\to\infty} N \leq N_0$. Thus, we have the feasible region for system (3) defined by

$$\Omega = \left\{(S, E, I, I_D, Q_2, R, D) \in \mathbb{R}_+^7 | 0 \leq N \leq N_0\right\}.$$

Our analysis will be based on the dynamics in $\Omega$. □

### 3.3. Disease-free equilibrium state and the basic reproduction number

The model has a disease-free equilibrium state

$$C^0 = \left(S^0, E^0, I^0, I_D^0, Q_2^0, R^0, D^0\right) = \left(S^0, 0, 0, 0, 0, 0, 0\right).$$

Following the next-generation matrix approach by van den Driessche and Watmough [35], we have

$$\mathcal{F} = \begin{pmatrix} 0 & \beta(1-\kappa) & \beta\eta(1-\kappa) & 0 \\ 0 & 0 & 0 & 0 \\ 0 & 0 & 0 & 0 \\ 0 & 0 & 0 & 0 \end{pmatrix} \quad \text{and}$$

$$\mathcal{V} = \begin{pmatrix} \sigma & 0 & 0 & 0 \\ -\sigma & \delta_1+\delta_2+\delta_3 & 0 & -q\phi \\ 0 & -\delta_1 & \rho & -(1-q)\phi \\ 0 & 0 & 0 & \phi \end{pmatrix}, \tag{8}$$

giving

$$\mathcal{R}_0 = \mathcal{R}_I + \mathcal{R}_{I_D} \quad \text{where} \quad \mathcal{R}_I = \frac{\beta(1-\kappa)}{(\delta_1+\delta_2+\delta_3)} \quad \text{and}$$

$$\mathcal{R}_{I_D} = \frac{\beta(1-\kappa)\delta_1\eta}{(\delta_1+\delta_2+\delta_3)\rho}. \tag{9}$$

$\mathcal{R}_I$ is the reproduction number contributed by the undetected infected class, $I(t)$ while $\mathcal{R}_{I_D}$ is the reproduction number contributed by the $I_D(t)$ class. The term $\frac{\beta(1-\kappa)}{(\delta_1+\delta_2+\delta_3)}$ means that the individuals in the undetected infected class $I(t)$ have contact with the susceptible class at a rate, $\beta(1-\kappa)$, and they will spend a mean time of $\frac{1}{(\delta_1+\delta_2+\delta_3)}$ within the undetected Infected class, $I(t)$. It can be noted that governmental action $\kappa$ will reduce the transmission rate, $\beta$. The term $\frac{\beta\eta\delta_1(1-\kappa)}{\rho(\delta_1+\delta_2+\delta_3)}$ means that some individuals within the undetected Infected class, $I(t)$ will be detected positive and isolated, at a testing rate of $\delta_1$ and spend a mean time $\frac{1}{(\delta_1+\delta_2+\delta_3)}$ within, $I(t)$ class. Thereafter, they will progress to the $I_D(t)$ class and spend an average infectious time of $\frac{1}{\rho}$ within the $I_D(t)$ class. The contact rate of such individuals is $\beta\eta\delta_1(1-\kappa)$, where $\eta$ is the modification parameter for the $I_D(t)$ class.

The following result follows from van den Driessche and Watmough [35].

**Theorem 3.** *The disease-free equilibrium for system (3) is locally asymptotically stable provided that $\mathcal{R}_0 < 1$.*

#### 3.3.1. Global stability of the disease-free equilibrium state

We shall now prove the global stability of the disease-free equilibrium point, $C^0$, whenever the reproduction number is less than unity.

**Theorem 4.** *The disease-free equilibrium for system (3) is globally asymptotically stable provided that $\mathcal{R}_0 < 1$.*

**Proof.** Using the approach in Shuai and van den Driessche [36], we construct the following Lyapunov function given by

$$\mathcal{L} = \left(\frac{1}{f} + \frac{\delta_1\eta}{f\rho}\right)[E+I] + \frac{\eta}{\rho}I_D + Q_2\left[\frac{q}{f} + \frac{\eta f(1-q)+q\delta_1}{f\rho}\right], \tag{10}$$

where $f = \delta_1+\delta_2+\delta_3$. Differentiating $\mathcal{L}$ yields

$$\dot{\mathcal{L}} = \left(\frac{1}{f} + \frac{\delta_1\eta}{f\rho}\right)[E+I]' + \frac{\eta}{\rho}I_D' + Q_2'\left[\frac{q}{f} + \frac{\eta f(1-q)+q\delta_1}{f\rho}\right]. \tag{11}$$

Substituting expressions for $E', I', I'_D, Q'_2$ leads to

$$\begin{aligned}\dot{\mathcal{L}} &= \left(\frac{1}{f}+\frac{\delta_1\eta}{f\rho}\right)[\lambda S + q\phi Q_2 - fI] + \frac{\eta}{\rho}[(1-q)\phi Q_2 + \delta_1 I - \rho I_D] \\ &\quad + \left[\frac{q}{f}+\frac{\eta f(1-q)+q\delta_1}{f\rho}\right][\Lambda - \phi Q_2] \\ &= \lambda S\left[\frac{1}{f}+\frac{\delta_1\eta}{f\rho}\right] - (I+\eta I_D) + \Lambda\left[\frac{q}{f}+\frac{\eta f(1-q)+q\delta_1}{f\rho}\right].\end{aligned} \tag{12}$$

Recall that $\lambda = \dfrac{\beta(1-\kappa)\left(I+\eta I_D\right)}{N}$ and $\mathcal{R}_0 = \beta(1-\kappa)\left[\frac{1}{f}+\frac{\delta_1\eta}{f\rho}\right]$. Hence, we obtain

$$\dot{\mathcal{L}} = \left[\frac{\mathcal{R}_0 S}{N} - 1\right](I+\eta I_D) + \Lambda\left[\frac{q}{f}+\frac{\eta f(1-q)+q\delta_1}{f\rho}\right]. \tag{13}$$

At the disease-free equilibrium $\Lambda = 0$ (there are no returnees being recruited into quarantine centers in Zimbabwe), then

$$\dot{\mathcal{L}} = \left[\frac{\mathcal{R}_0 S}{N} - 1\right](I+\eta I_D). \tag{14}$$

Then, it follows that

$$\dot{\mathcal{L}} \le (\mathcal{R}_0 - 1)(I+\eta I_D), \tag{15}$$

since $\frac{S}{N} \le 1$. This implies that $\dot{\mathcal{L}} \le 0$ provided that $\mathcal{R}_0 \le 1$ and $\dot{\mathcal{L}} = 0$ iff $I = I_D = E = Q_2 = 0$. Hence, by applying LaSalle's invariance principle [37] it suffices to conclude that the disease-free equilibrium, $C^0$ is globally asymptotically stable provided $\mathcal{R}_0 < 1$ and unstable otherwise. This concludes the proof. □

### 3.4. Sensitivity analysis of $\mathcal{R}_0$.

We perform sensitivity analysis to establish which parameters have a positive or negative effect on the $\mathcal{R}_0$ expression given in (9). We use the following normalized forward sensitivity index formula as given in [38].

$$\Gamma_\omega^{\mathcal{R}_0} = \frac{\partial \mathcal{R}_0}{\partial \omega} \times \frac{\omega}{\mathcal{R}_0}, \tag{16}$$

where $\omega$ is the parameter of interest. Below are sensitivity indices of $\mathcal{R}_0$ with respect to each of its parameters.

$$\begin{cases} \Gamma_\beta^{\mathcal{R}_0} = 1, \quad \Gamma_\eta^{\mathcal{R}_0} = \dfrac{\delta_1\eta}{\delta_1\eta+\rho}, \quad \Gamma_\kappa^{\mathcal{R}_0} = -\dfrac{\kappa}{1-\kappa}, \\ \qquad\qquad \Gamma_\rho^{\mathcal{R}_0} = -1 + \dfrac{\rho}{\delta_1\eta+\rho}, \\ \Gamma_{\delta_1}^{\mathcal{R}_0} = \delta_1\left(\dfrac{\eta}{\delta_1\eta+\rho} - \dfrac{1}{\delta_1+\delta_2+\delta_3}\right), \quad \Gamma_{\delta_2}^{\mathcal{R}_0} = -\dfrac{\delta_2}{\delta_1+\delta_2+\delta_3}, \\ \qquad\qquad \Gamma_{\delta_3}^{\mathcal{R}_0} = -\dfrac{\delta_3}{\delta_1+\delta_2+\delta_3}. \end{cases} \tag{17}$$

Here, the sensitivity indices for the given parameters as presented in (17) only indicate the direction of influence without quantifying the given parameter's influence. We note that the parameters $\beta$ and $\eta$ have a direct proportional relationship with $\mathcal{R}_0$, with $\mathcal{R}_0$ most sensitive to changes in $\beta$. An increase (or decrease) in either of these parameters will result in an equivalent increase (or decrease) in the value of $\mathcal{R}_0$. Parameters $\kappa$, $\rho$, $\delta_2$ and $\delta_3$ have an inversely proportional relationship with $\mathcal{R}_0$, an increase in the values of these parameters will lead to a decrease in the value of $\mathcal{R}_0$. However, putting down measures that will increase the value of $\delta_3$ is unethical. Thus, measures such as increased surveillance and isolation of infected individuals (increase in $\rho$) and enforcing governmental actions such as wearing of face masks, use of sanitizers, social distancing, etc. (increase in $\kappa$) will be of great help in curtailing the spread of COVID-19. Interestingly, $\Gamma_{\delta_1}^{\mathcal{R}_0} < 0$ when $\rho > \left(2\delta_1+\delta_2+\delta_3\right)\eta$ and $\Gamma_{\delta_1}^{\mathcal{R}_0} > 0$ when $\rho < \left(2\delta_1+\delta_2+\delta_3\right)\eta$. This entails that the detection rate on infected individuals will reduce the value of $\mathcal{R}_0$ provided there is an adequate amount of time spent in isolation for infected individuals.

## 4. Numerical simulations

In this section, we perform numerical simulations of system (3). We consider a case study of COVID-19 transmission dynamics in Zimbabwe. The model in the present study has many parameters whose values must be ascertained to properly capture the COVID-19 transmission dynamics in Zimbabwe for the period 30th of March 2020 up to the 30th of June 2020. To capture the COVID-19 dynamics in Zimbabwe for this period, we fit the model to the observed COVID-19 data. We assign reasonable ranges from which parameter values are chosen and we obtain parameter values that give the best fit. These parameters are used to perform our numerical simulations. We also carry out some forecasting of the disease dynamics under certain conditions within the framework of the objectives of the study. For instance, we investigate the long-term impact of governmental actions such as lockdowns, social distancing, closure of schools and universities, etc.

We consider COVID-19 data starting from the 30th of March 2020 (day 1), when the first lockdown was instituted in Zimbabwe, up to the 30th of June 2020 (day 93). Important timelines for the management and control of COVID-19 in Zimbabwe, as given by the government authorities, are as follows:

1. declaration of state of disaster on the 17th of March 2020 [39],
2. 1st lockdown instituted on the 30th of March 2020 [39],
3. 2nd lockdown instituted on the 6th of May 2020 [40],
4. 3rd lockdown instituted on the 20th of May 2020 for an indefinite period covering the drafting of this manuscript [41].

We tabulate the data for COVID-19 cases in three parts, namely: (i) the period covering the 1st lockdown (see Table 1), (ii) the period before the massive surge of returnees (see Table 2. This period covers all of the 1st lockdown period, all of the 2nd lockdown period and part of the initial stages of the 3rd indefinite lockdown period), and (iii) the period after the massive surge of returnees (see Table 3. This period covers most of the 3rd indefinite lockdown period).

To estimate our unknown model parameters and unpack the underlying dynamics of the COVID-19 pandemic in Zimbabwe, we use the curve-fitting process to quantify the trend of the outcomes of this pandemic. Here, we fit the equations of approximating curves to the available raw field data on COVID-19 dynamics in Zimbabwe. Generally, it will be observed that the fitting curves for any given data set are not unique. Thus, a curve with minimum possible deviation from all the data points will be desired. The least squares curve fit routine (lsqcurvefit) in Matlab with optimization is used to estimate our unknown model parameters. The procedure requires that a lower and an upper bound be set from which estimates of the unknown parameter values are obtained. Thus, using the available data on cumulative cases for COVID-19 in Zimbabwe over a defined time frame, $t_{i-1} \le t \le t_i$ (where $t_{i-1}$ and $t_i$ indicate the beginning and end of the time interval, respectively), we estimate using the function

$$C(t) = \int_{t_{i-1}}^{t_i} \left[(1-q)\phi Q_2(t) + \delta_1 I(t)\right] dt. \tag{18}$$

We applied the ordinary least squares (OLS), which is a standard approach in regression analysis, to approximate the solution of overdetermined systems by minimizing the sum of the squares of the residuals made in the results of each equation while fitting our Model to Eq. (18). The OLS is advantageous as it provides a rationale for placing the line of best fit, taking into account the input data and the model under parameterization of its validation process while giving the smallest sum of squares of variance [10,43]. Also, the OLS algorithms allow researchers to estimate unknown model parameter values by specifying a lower bound and an upper bound from which the set of estimated parameter values are generated once the algorithm obtains a line of best fit. Applying OLS to our model, we validate the system (3) by fitting it to the data, which yields Table 4 using the least square regression

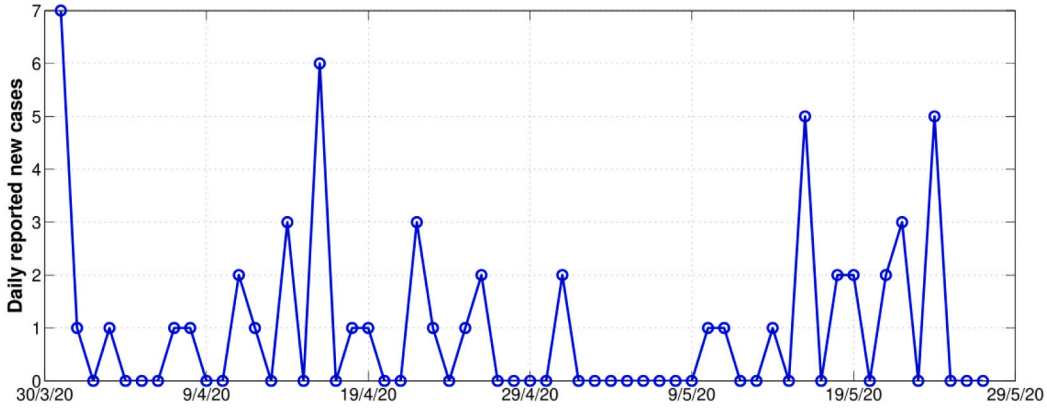


**Fig. 3.** Daily reported new cases in Zimbabwe starting on the 30th of March 2020 and ending on the 27th of May 2020.

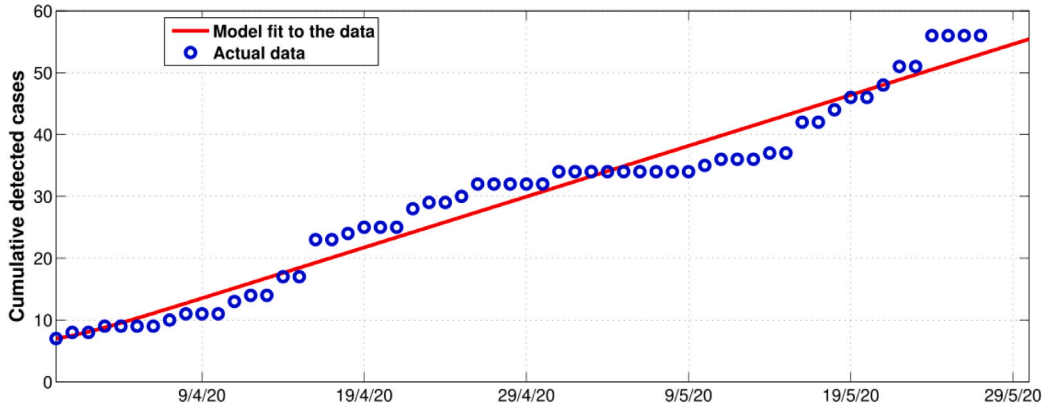


**Fig. 4.** Model system (3) fitted to data for cumulative COVID-19 cases in Zimbabwe before the massive surge of returnees starting from the 30th of March 2020 and ending on the 27th of May 2020. See Table 2. This period covers the whole of the 1st and 2nd lockdown period and partly covers the initial stages of the 3rd indefinite lockdown period. The *blue circles* indicate the actual data, and the *solid red line* indicates the model fit to the data. The initial conditions obtained from data fitting are as follows: $N(0) = 14 \times 10^6$; $S(0) = N(0) - E(0) - I(0) - I_D(0) - Q_2(0) - R(0)$; $E(0) = 0$; $I(0) = 0$; $I_D(0) = 7$; $Q_2(0) = \Lambda = 61$; $R(0) = 0$; $D(0) = 1$ where $t = 0$ corresponds to the 30th of March 2020 for this case.

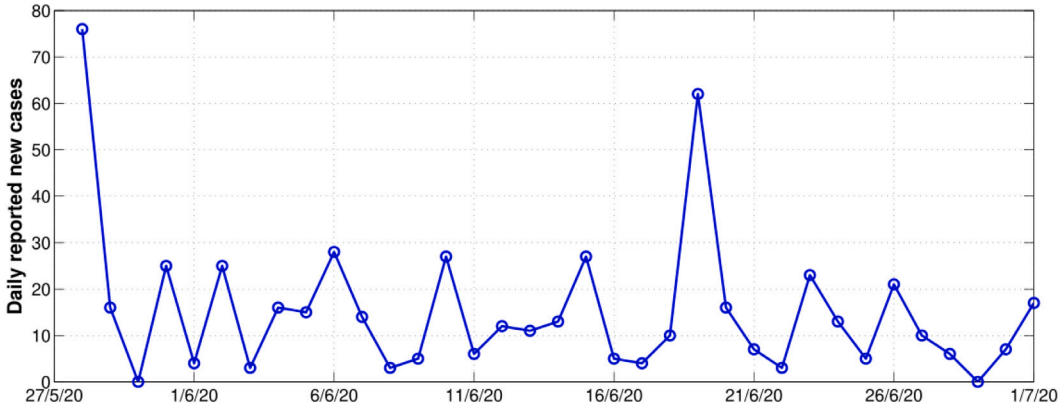


**Fig. 5.** Daily reported new cases in Zimbabwe starting on the 27th of May 2020 and ending on the 30th of June 2020.

**Table 1**
Confirmed COVID-19 cases in Zimbabwe before lockdown [42].

| Date | 20/3/20 | 21/3/20 | 22/3/20 | 23/3/20 | 24/3/20 | 25/3/20 | 26/3/20 | 27/3/20 |
|---|---|---|---|---|---|---|---|---|
| Total cases | 1 | 3 | 3 | 3 | 3 | 3 | 3 | 5 |
| Date | 28/3/20 | 29/3/20 | | | | | | |
| Total cases | 7 | 7 | | | | | | |

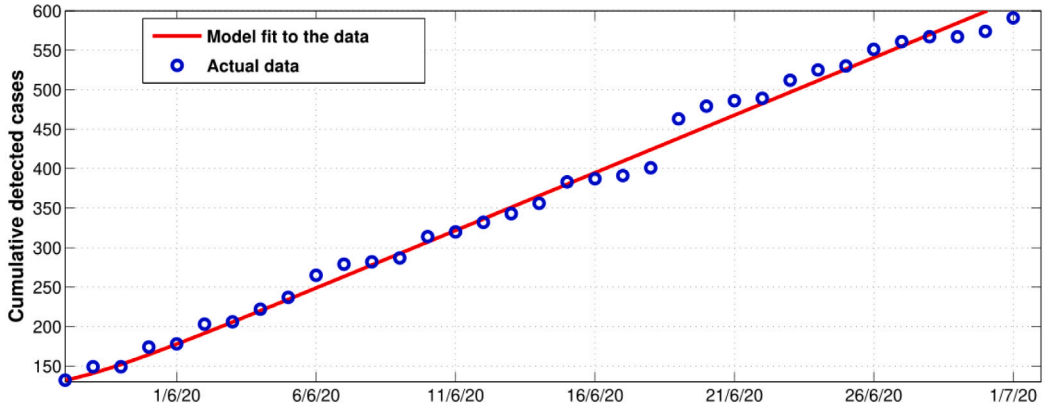


**Fig. 6.** Model system (3) fitted to data for cumulative COVID-19 cases in Zimbabwe after the massive surge of returnees starting from the 27th of May 2020 and ending on the 30th of June 2020 (see Table 3). This period covers most of the 3rd indefinite lockdown period. The *blue circles* indicate the actual data, and the *solid red line* indicates the model fit to the data. The initial conditions obtained from data fitting are as follows: $N(0) = 14 \times 10^6$; $S(0) = N(0) - E(0) - I(0) - I_D(0) - Q_2(0) - R(0)$; $E(0) = 50$; $I(0) = 0$; $I_D(0) = 132$; $Q_2(0) = \Lambda = 1000$; $R(0) = 25$; $D(0) = 4$ where $t = 0$ corresponds to the 27th of May 2020 for this case.

**Table 2**
Confirmed COVID-19 cases in Zimbabwe before massive surge of returnees. This period covers the whole of the 1st lockdown period, the whole of the 2nd lockdown period and partly covers the initial stages of the 3rd indefinite lockdown period [42].

| | | | | | | | | |
|---|---|---|---|---|---|---|---|---|
| Date | 30/3/20 | 31/3/20 | 1/4/20 | 2/4/20 | 3/4/20 | 4/4/20 | 5/4/20 | 6/4/20 |
| Total cases | 7 | 8 | 8 | 9 | 9 | 9 | 9 | 10 |
| Date | 7/4/20 | 8/4/20 | 9/4/20 | 10/4/20 | 11/4/20 | 12/4/20 | 13/4/20 | 14/4/20 |
| Total cases | 11 | 11 | 11 | 13 | 14 | 14 | 17 | 17 |
| Date | 15/4/20 | 16/4/20 | 17/4/20 | 18/4/20 | 19/4/20 | 20/4/20 | 21/4/20 | 22/4/20 |
| Total cases | 23 | 23 | 24 | 25 | 25 | 25 | 28 | 29 |
| Date | 23/4/20 | 24/4/20 | 25/4/20 | 26/4/20 | 27/4/20 | 28/4/20 | 29/4/20 | 30/4/20 |
| Total cases | 29 | 30 | 32 | 32 | 32 | 32 | 32 | 34 |
| Date | 1/5/20 | 2/5/20 | 3/5/20 | 4/5/20 | 5/5/20 | 6/5/20 | 7/5/20 | 8/5/20 |
| Total cases | 34 | 34 | 34 | 34 | 34 | 34 | 34 | 34 |
| Date | 9/5/20 | 10/5/20 | 11/5/20 | 12/5/20 | 13/5/20 | 14/5/20 | 15/5/20 | 16/5/20 |
| Total cases | 35 | 36 | 36 | 36 | 37 | 37 | 42 | 42 |
| Date | 17/5/20 | 18/5/20 | 19/5/20 | 20/5/20 | 21/5/20 | 22/5/20 | 23/5/20 | 24/5/20 |
| Total cases | 44 | 46 | 46 | 48 | 51 | 51 | 56 | 56 |
| Date | 25/5/20 | 26/5/20 | | | | | | |
| Total cases | 56 | 56 | | | | | | |

technique. This technique minimizes the sum of the squared residuals given by:

$$\mathcal{R}(\Psi) = \sum_{i=1}^{n} \left( p_{t_i}(\Psi) - \tilde{p}_{t_i} \right)^2.$$

Here, $\Psi$ represents all the model parameters in Table 4, $n$ is the total number of data points used for the fitting process, $p_{t_i}(\Psi)$ and $\tilde{p}_{t_i}$ are the Zimbabwe cumulative COVID-19 cases of infected individuals by our model predictions and the actual reported data for the time frame under investigation respectively (see Figs. 3–6).

### 4.1. Epidemiological parameter estimation

Under this section, we ascertain epidemiological parameter values used for conducting numerical simulations. We use the available expanding literature on COVID-19 dynamics and the Zimbabwe COVID-19 data fitting. Immigration of exposed individuals ($\Lambda$) is estimated for the periods before and after the massive surge of returnees. The mandatory quarantine period for returnees is 21 days, with some individuals escaping from quarantine before this period lapses. Thus, we choose a range of between 14 to 21 days and set the mean duration of quarantine to be $\phi^{-1} = 14$ days [44]. The proportion, $q$, of those escaping from quarantine facilities is chosen to fall within the range $[0.00138, 0.025]$ per day [44,45]. The proportion of the detected and isolated individuals who progress into the recovered class $R(t)$ is considered to be within the range $d = [0.26, 0.5]$, drawn from the work done in [44,46]. Following [5,47], we assign the range for the governmental action parameter $\kappa$ as $\kappa \in [0.4239, 0.8478]$. Further, the remaining parameter values are estimated from the COVID-19 data fit, which are the disease transmission rate; $\beta = 0.5643$, modification parameter; $\eta = 0.7015$, detection rate of infected individuals; $\delta_1 = 4.0816 \times 10^{-7}$ and the mean duration period for isolation of detected individuals is $\rho^{-1} = 10$ days. We provide a summary of the description of parameters, ranges, and values used in Table 4.

### 4.2. Sensitivity analysis

According to Marino [53], we note that in any mathematical modeling exercise, the model variables and parameters are uncertain, making it difficult to quantify. Also, sensitivity analysis can be carried out over time intervals with no particular time frame under investigation for exploratory purposes. For instance, the exact number of exposed returnees remains difficult to accurately measure considering some unaccounted cases of individuals who skip the border. More generally, describing a phenomenon using models is often linked with incomplete available knowledge due to a lack of analogous experimental measures.

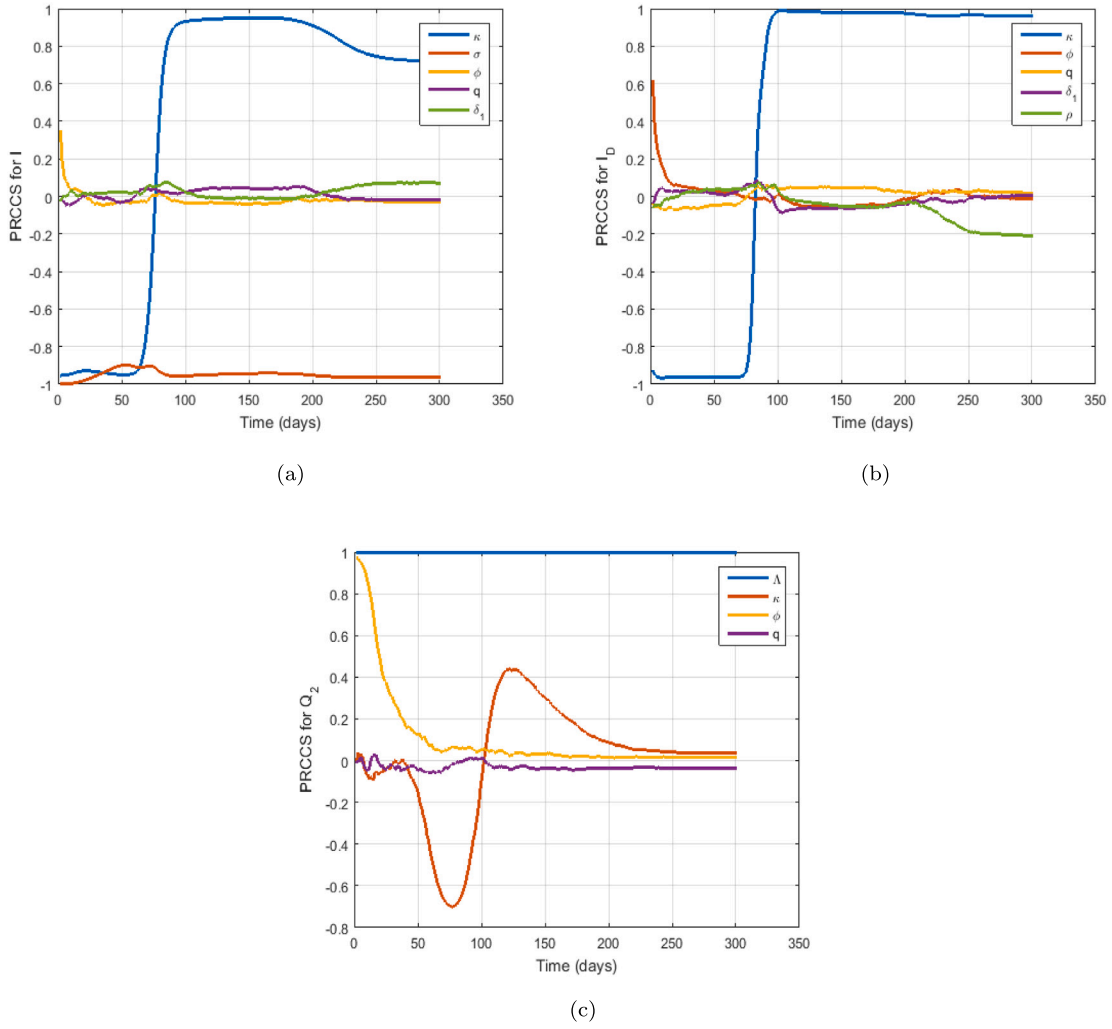


**Fig. 7.** Plots of PRCC values showing the effects of long-term dynamics before surging for parameter values on COVID-19 disease in Zimbabwe over time for (a) parameters $\kappa$, $\sigma$, $\phi$, $q$, $\delta_1$ against $I$. (b) parameters $\kappa$, $\phi$, $q$, $\delta_1, \rho$ against $I_D$. (c) parameters $\Lambda$, $\kappa$, $\phi$, $q$ against $Q_2$.

**Table 3**
Confirmed COVID-19 cases in Zimbabwe after massive surge of returnees. This period covers most of the 3rd indefinite lockdown period [42].

| | | | | | | | | |
|---|---|---|---|---|---|---|---|---|
| Date | 27/5/20 | 28/5/20 | 29/5/20 | 30/5/20 | 31/5/20 | 1/6/20 | 2/6/20 | 3/6/20 |
| Total cases | 132 | 149 | 149 | 174 | 178 | 203 | 206 | 222 |
| Date | 4/6/20 | 5/6/20 | 6/6/20 | 7/6/20 | 8/6/20 | 9/6/20 | 10/6/20 | 11/6/20 |
| Total cases | 237 | 265 | 279 | 282 | 287 | 314 | 320 | 332 |
| Date | 12/6/20 | 13/6/20 | 14/6/20 | 15/6/20 | 16/6/20 | 17/6/20 | 18/6/20 | 19/6/20 |
| Total cases | 343 | 356 | 383 | 387 | 391 | 401 | 463 | 479 |
| Date | 20/6/20 | 21/6/20 | 22/6/20 | 23/6/20 | 24/6/20 | 25/6/20 | 26/6/20 | 27/6/20 |
| Total cases | 486 | 489 | 512 | 525 | 530 | 551 | 561 | 567 |
| Date | 28/6/20 | 29/6/20 | 30/6/20 | | | | | |
| Total cases | 567 | 574 | 591 | | | | | |

Hence, we chose only the most important parameters and/or state variables in relation to the subject/aim of the study. It is important to note that as indicated in [53], all parameters that have partial rank correlation coefficients (PRCCs) between −0.2 to 0.2 are considered to be less sensitive, though this can be further justified by the calculation of the associated P-values in further study. Sensitivity analyses were done using the state variables: the undetected individuals $I$, detected and isolated individuals $I_D$ and the exposed individuals in quarantine $Q_2$ to determine the most influential parameters; $\Lambda$, $\rho$, $\delta_1$, $q$, $\phi$, $\kappa$ and $\sigma$ on the increase/decrease of the escapee individuals on COVID-19 disease transmission dynamics. We aim to determine the impact of these parameters against the state variable of choice for their short and long-term transmission dynamics for our model by considering their Partial Rank Correlation Coefficients (PRCC) values over the modeling time. This will help us to quantify the role of escapees on SARS-CoV-2 transmissions before and after the surge of the disease. Here, we consider the sensitivity analysis of these parameters before and after a surge of COVID-19, as presented in the subsections below.

#### 4.2.1. Sensitivity analysis before surge

Some parameters from Table 1 are used to carry out global uncertainty sensitivity analysis of model system (3) with the combination

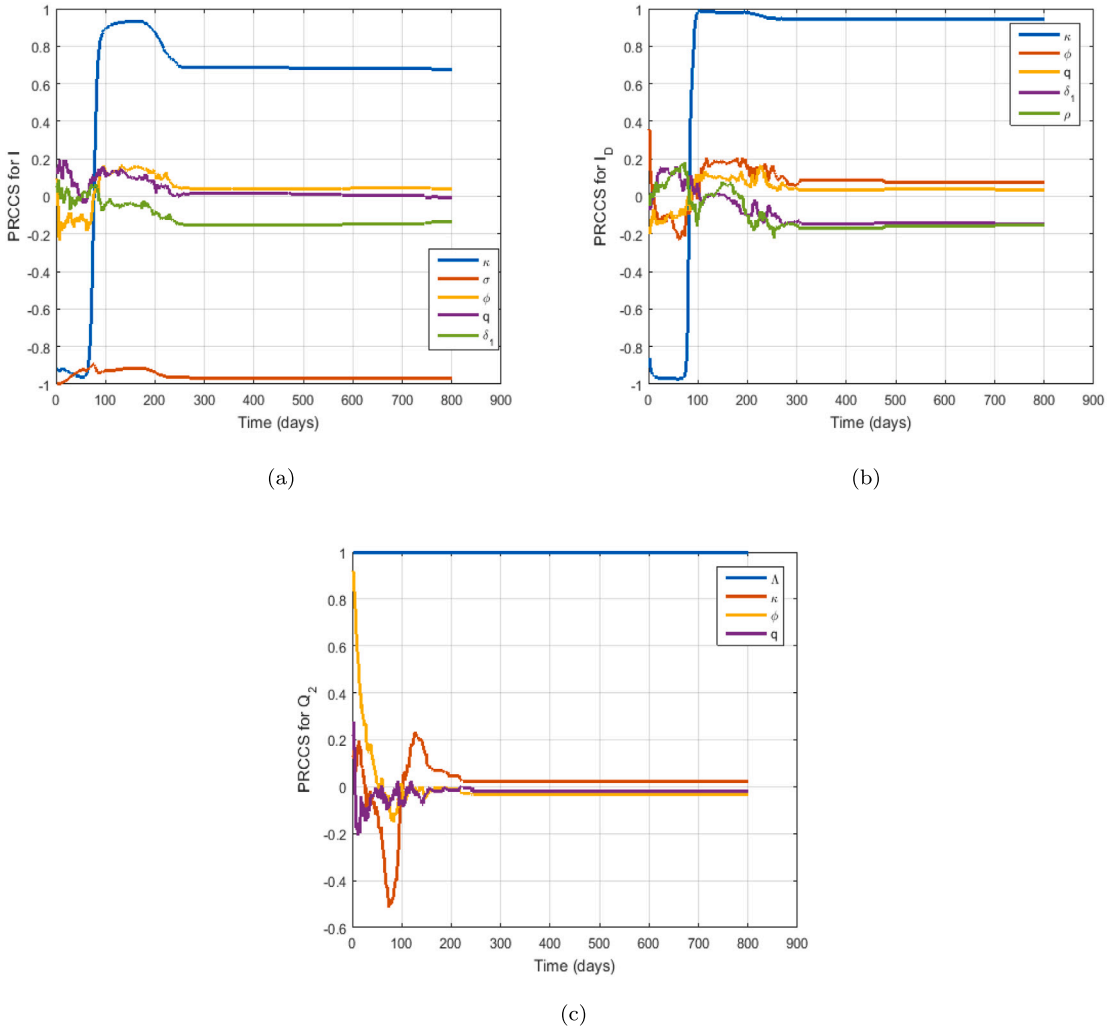


**Fig. 8.** Plots of PRCC value showing the effects of long-term dynamics before surging for parameter values on COVID-19 disease in Zimbabwe over time for (a) parameters $\kappa$, $\sigma$, $\phi$, $q$, $\delta_1$ against $I$. (b) parameters $\kappa$, $\phi$, $q$, $\delta_1, \rho$ against $I_D$. (c) parameters $\Lambda$, $\kappa$, $\phi$, $q$ against $Q_2$.

**Table 4**
Description of parameters in system (3) using data for Table 2.

| Description | Symbol | Range | Baseline value | Source |
|---|---|---|---|---|
| Disease transmission rate | $\beta$ | $[0.4, 1]$ | 0.5643 | Data fit |
| Governmental action | $\kappa$ | $[0.4239, 0.8478]$ | 0.55 | [5,47] |
| Modification factor | $\eta$ | $[0.4, 1]$ | 0.7015 | Data fit |
| Mean incubation period | $\sigma^{-1}$ | 5–6 days | 5 | [48,49] |
| Mean duration in quarantine | $\phi^{-1}$ | 14 days | 14 | [46] |
| Proportion of escapees | $q$ | $[0.00138, 0.025]$ day$^{-1}$ | 0.00138 | [44,45] |
| Detection rate of infected individuals | $\delta_1$ | $[0, 0.7]$ day$^{-1}$ | $4.0861 \times 10^{-7}$ | Data fit |
| Recovery rate of undetected individuals | $\delta_2$ | $[0.0752, 0.1370]$ day$^{-1}$ | 0.0795 | [50,51] |
| Disease-related death for infected individuals | $\delta_3$ | $[0.03, 0.04]$ day$^{-1}$ | 0.04 | [52] |
| Mean duration in isolation | $\rho^{-1}$ | $[0.03, 0.2]$ days | 0.1 | Data fit |
| Proportion of isolated individuals who recovers | $d$ | $[0.26, 0.5]$ day$^{-1}$ | 0.26 | [44,45] |
| Immigration of exposed individuals | $\Lambda$ | $[50, 100]$ day$^{-1}$ | 61 | Data fit |

of Latin Hypercube Sampling (LHS) and the partial rank correlation coefficients (PRCC) as in [53]. A sample size of $N = 500$ with a unit step of 1 is used to implement the simulations in this subsection for both the short-term and long-term dynamics of the disease and their results are depicted in Figs. 7 and 8 respectively. The basic reproduction number for this case was found to be $\mathcal{R}_0 = 2.1$.

*Short term predictions dynamics*

In Fig. 7(a), we observe that the parameter, $\kappa$ being the governmental role actions during the pandemic, is negatively correlated at the onset of the disease and becomes positively correlated from $t = 10$ to $t = 300$ days. Meanwhile, the parameter $\sigma$ is negatively correlated over the modeling time with respect to the undetected individuals, $I(t)$. Also, Fig. 7(b) gives a similar trend to what we observe in Fig. 7(a), only that the parameter $\phi$ becomes positively correlated at the onset of the epidemic and diminishes as time progresses against the exposed individuals in quarantine, $I_D(t)$. On the other hand, we observe in Fig. 7(c) that the immigration rate, $\Lambda$, has a perfect strong correlation, while the parameter, $\phi$, is positive and diminishes with time. The parameter, $\kappa$, has a negative correlation from the time $t = 0$ to time $t = 100$ and a positive correlation from $t > 100$ and becomes less significant after $t > 170$.

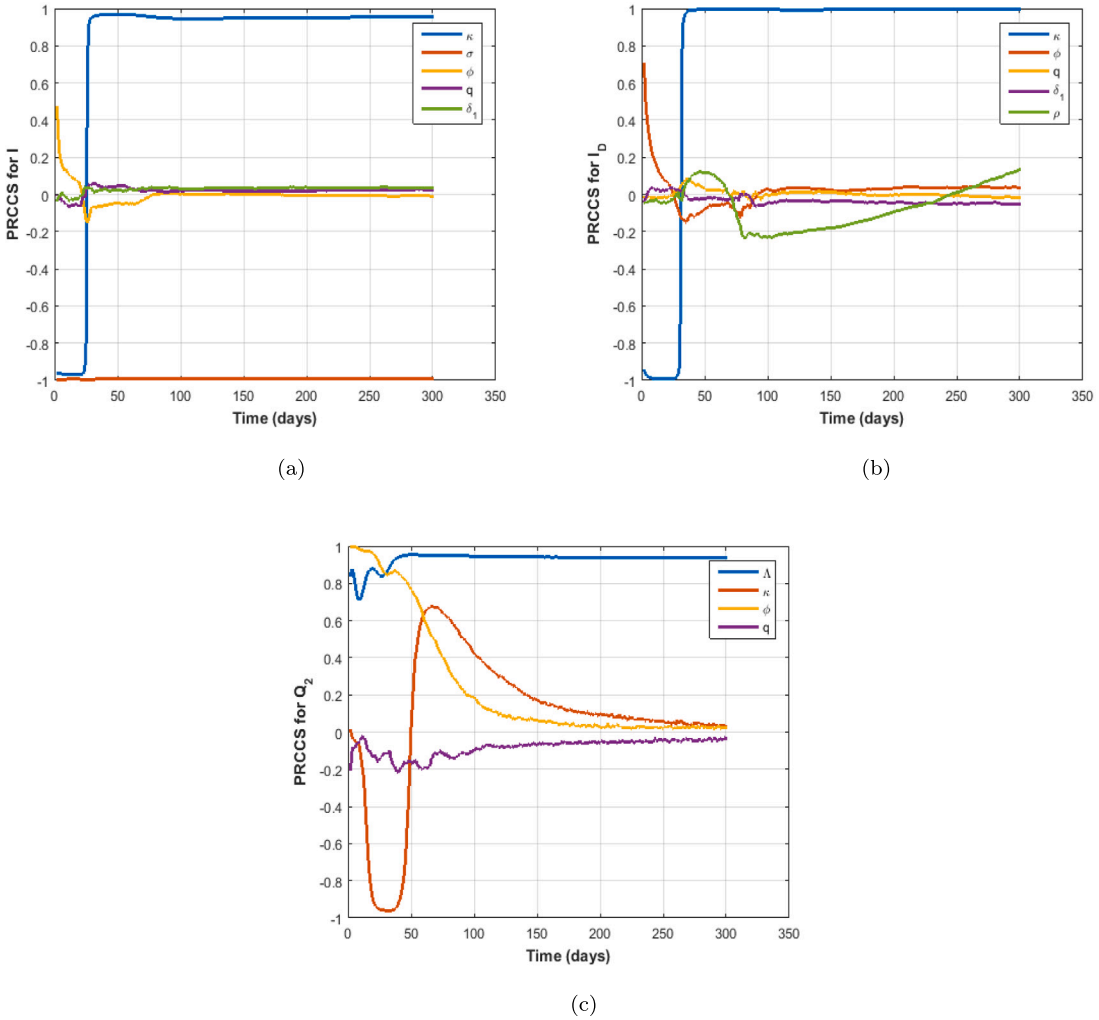


**Fig. 9.** Plots of PRCC values showing the effects of short-term dynamics after surging for parameter values on COVID-19 disease in Zimbabwe over time for (a) parameters $\kappa$, $\sigma$, $\phi$, $q$, $\delta_1$ against $I$. (b) parameters $\kappa$, $\phi$, $q$, $\delta_1, \rho$ against $I_D$. (c) parameters $\Lambda$, $\kappa$, $\phi$, $q$ against $Q_2$.

*Long term predictions dynamics*

We observe in Figs. 8(a) and 8(b) that at the onset of the disease, the parameter $\kappa$ has a negative correlation and eventually becomes positive after time $t = 80$ for the undetected and exposed individuals in quarantine. Further, in Fig. 8(c) $\kappa$ is negatively correlated to the $Q_2$ individuals and becomes positive after 90 days. The parameters, $\sigma$ and $\Lambda$ are strongly negative and positive correlated respectively against $I$ and $Q_2$ as observed in Figs. 8(a) and 8(c) respectively. Biologically, this signifies that an increase in the immigration rate, $\Lambda$, will increase the number of quarantined individuals, while a decrease in $\sigma$ will lead to a decrease in the number of undetected individuals before a surge.

### 4.2.2. Sensitivity analysis after surge

We also use Table 3, and a sample size of $N = 500$ runs with a unit step to perform sensitivity analysis under this subsection. Short-term results are depicted in Fig. 9 while long-term results are depicted in Fig. 10. The basic reproduction number for this case is found to be $\mathcal{R}_0 = 2.8$.

*Short term predictions dynamics*

In Figs. 9(a)–9(c), we observe that the parameter, $\kappa$, has a negative correlation from time $t = 0$ to $t = 50$ and thereafter it becomes positively correlated against the state variables $I$, $I_D$ and $Q_2$. This implies that an increase in governmental role action, such as implementing lock-downs and wearing masks, needs to be continued after the first surge to control the disease effectively. On the other hand, the immigration rate, $\Lambda$, has a strong positive correlation over time as seen in Fig. 9(c) while the parameter $\sigma$ has a strong perfect negative correlation against the state variable, $I_D$. Also, as seen before a surge, an increase in the immigration rate during COVID-19 will result in more infections in a wholly susceptible population. On the other hand, the mean duration of quarantine parameter $\phi$ does not strongly impact the class, $I_D$, as time increases as it becomes positive and diminishes.

*Long term predictions dynamics*

A similar trend is also seen in Figs. 10(a) and 10(c) for the parameter $\kappa$. It has negative PRCC values from the first 30 days and positive PRCC values for $t > 40$. Also, in Figs. 10(a)–10(c), we observe that the mean duration in quarantine, $\phi$, has a positive PRCC value and diminishes as time progresses. The mean duration of incubation is not significant at the onset after the surge but becomes prominently positively correlated after time $t > 200$. In addition, the immigration rate, $\Lambda$, has a perfect positive correlation PRCC value over the modeling time.

### 4.3. Effects of varying parameters $q$ and $\kappa$ on $I(t)$

We investigate the impact of parameters $q$ and $\kappa$ on the number of undetected infected individuals, $I(t)$. The impact of $q$ is considered for the period before and after the massive surge of returnees, whereas the impact of $\kappa$ is considered for the period after the massive surge of returnees.

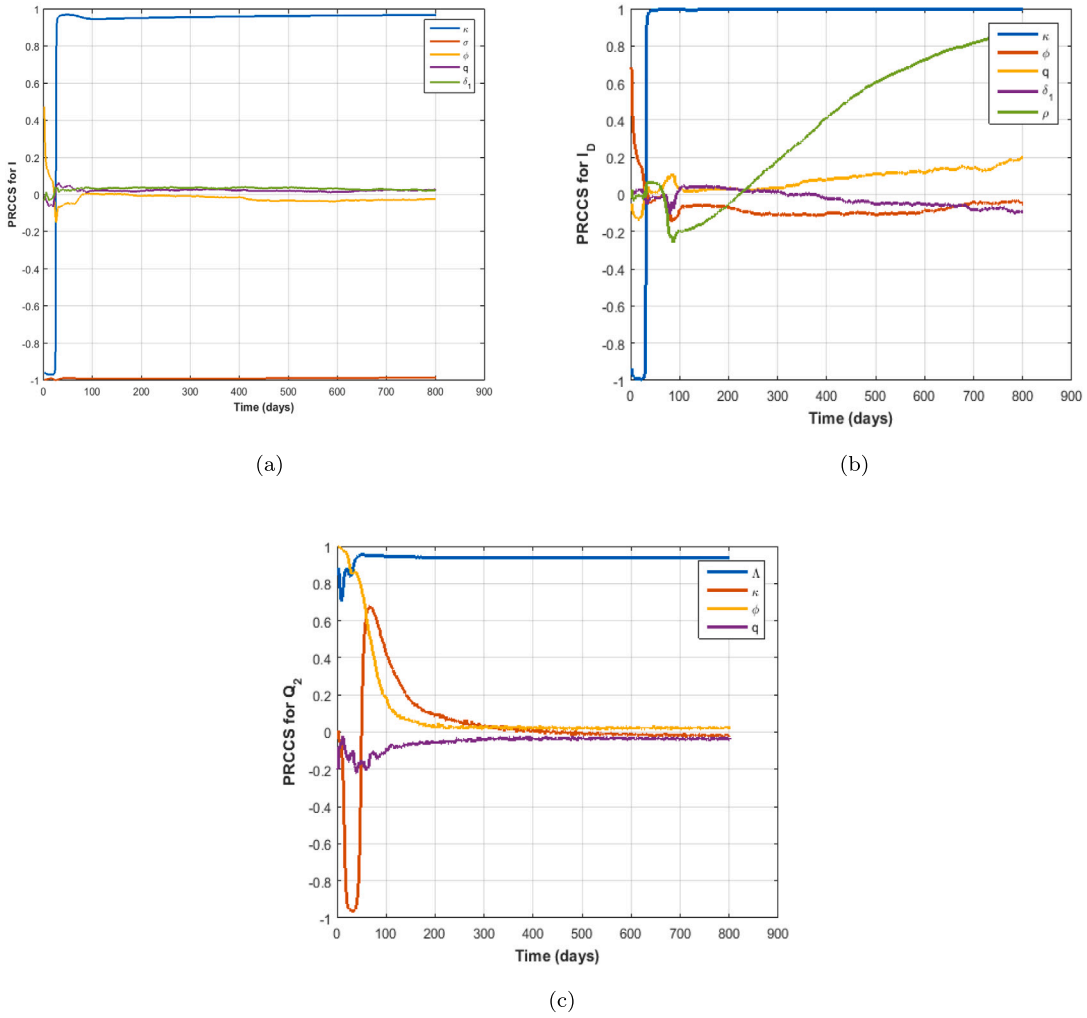


**Fig. 10.** Plots of PRCC value showing the effects of long-term dynamics after surging for parameter values on COVID-19 disease in Zimbabwe over time for (a) parameters $\kappa$, $\sigma$, $\phi$, $q$, $\delta_1$ against $I$. (b) parameters $\kappa$, $\phi$, $q$, $\delta_1, \rho$ against $I_D$. (c) parameters $\Lambda$, $\kappa$, $\phi$, $q$ against $Q_2$.

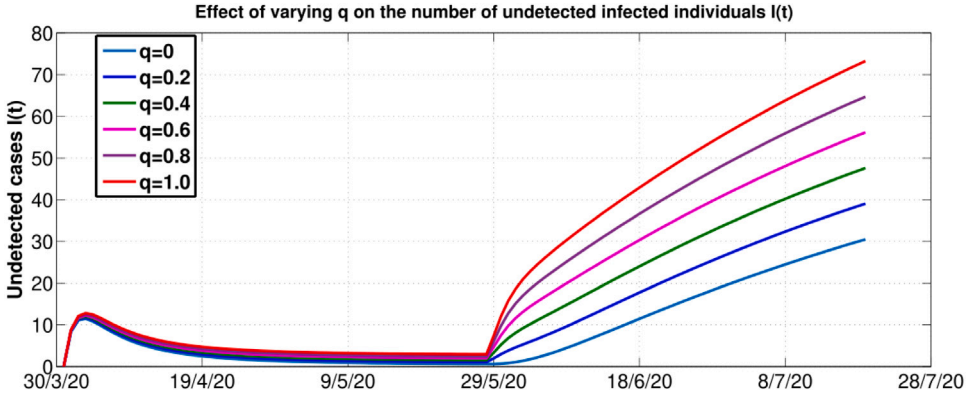


**Fig. 11.** Effect of varying $q$ on the number of undetected individuals.

We observe from Fig. 11 that the variation of $q$ before the massive surge of returnees has less impact than the period after the massive surge of returnees. We note that an increase in the value of $q$ fuels the presence of undetected infected individuals. A 20% increase in the value of $q$ increases 10 more daily undetected infected cases, which will be responsible for any undetected local transmissions. Fig. 12 illustrates that increased governmental action results in fewer undetected infected individuals. We observe that a 20% increase in the intensity of $\kappa$ will result in approximately a maximum drop of 15 daily undetected cases. This reflects the importance of ensuring adherence to measures put in place by the government to help control this pandemic.

### 4.4. Effects of parameters on $\mathcal{R}_0$

We use contour plots to investigate the effects of some crucial parameters on $\mathcal{R}_0$. These results support the analytical findings of the

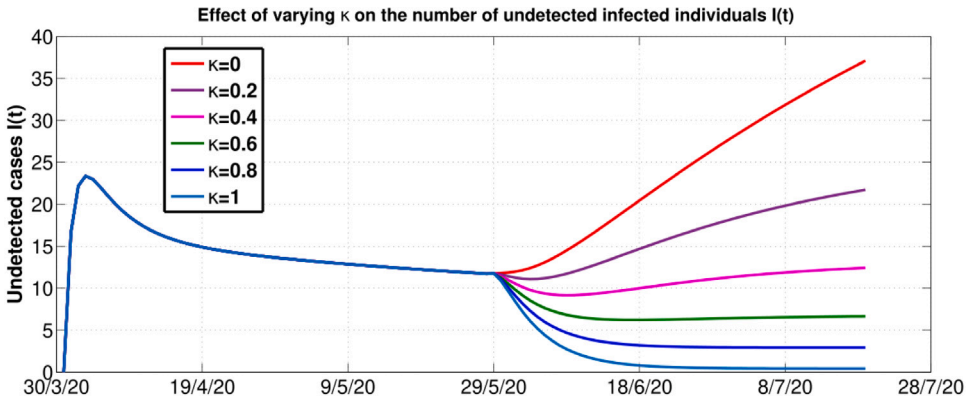


**Fig. 12.** Effect of varying $k$ after the 27th of May 2020 on the number of undetected individuals.

sensitivity analysis done on $\mathcal{R}_0$. Figs. 13(a) and 13(c) show that an increase in the rate of implementation of governmental actions ($\kappa$) results in a decrease in the value of $\mathcal{R}_0$. Also, we note that the instituted governmental policy of isolating detected infected individuals reduces $\mathcal{R}_0$. Fig. 13(b) shows that an increase in the proportion of escapees, $q$, will increase the disease transmission rate ($\beta$). This entails more infectious individuals due to escapees, which will, in turn, increase local COVID-19 transmission.

### 4.5. Effects of different lockdown measures

We investigate the impact of different lockdown scenarios on the COVID-19 dynamics in Zimbabwe.

Figs. 14, 15, 16, and 17 illustrate the impact of different lockdown strategies to curb the spread of the COVID-19 pandemic. Results show that the longer the period the lockdown is in force, the more reduction in the number of cases observed. However, this is usually accompanied by an economic impact that may be difficult to endure. Thus, some trade-offs between the economy and the infection would need to be taken care of to ensure human life is preserved at a bearable economic cost. Besides the length of the lockdown period, we also note that the timing of the lockdown implementation is crucial in the fight against the COVID-19 pandemic. A long delay in implementing the lockdown can fail to minimize the rising number of infections. This also can lead to the number of infections increasing above the threshold healthcare capacity, resulting in an otherwise avoidable loss of life. Lastly, Fig. 18 estimates the projected time for reaching peak cases of COVID-19 in the presence of the current dynamics of escapees. We observe that the peak number of cases will be reached by approximately the beginning of October 2020.

## 5. Conclusions

In this research paper, we investigate the impact of individuals escaping from quarantine centers on the dynamics of COVID-19 transmission in Zimbabwe. To analyze this, we employ a deterministic compartmental model and subject it to a comprehensive examination utilizing tools from the extensive field of mathematical epidemiology. Our study includes determining and exploring the model's reproduction number, which is pivotal in assessing the model's stability. We establish that the disease-free equilibrium is locally and globally asymptotically stable provided that $\mathcal{R}_0 < 1$. Global stability of the disease-free equilibrium poses a more robust condition and suggests that even if there are initial infections, COVID-19 is not expected to persist within the population in the long run. Based on this, sufficient control measures and interventions are needed to control and eliminate the pandemic.

Our numerical simulations yield several key findings. Firstly, we observe that an increase in the number of escapees from quarantine centers leads to a higher rate of local transmissions, resulting in more individuals contracting the infection. Secondly, our research underscores the necessity of governmental actions exceeding a threshold of 65% to effectively contain the spread of COVID-19 in Zimbabwe. This highlights the critical importance of implementing measures that enhance compliance with government-introduced intervention strategies to combat the infection. Thirdly, our sensitivity analysis reveals a strong positive correlation between the escapee parameter, denoted as "$q$", and the daily immigration rate, represented by "$\Lambda$", with the number of newly reported daily COVID-19 infections. This correlation signifies that more escapees contribute to increased local transmissions and prolonged disease duration. As a result, implementing mitigation measures such as improving surveillance in quarantine centers becomes crucial to reducing the number of escapees.

While our research offers valuable insights, it does have limitations. Notably, we did not account for vital dynamics as the disease approaches its peak. Incorporating vital dynamics in future studies is imperative for a more comprehensive understanding of the disease's dynamics. Also, the study did not account for the potential evolution of the COVID-19 virus or the emergence of new variants, which can impact transmission dynamics and government regulations. Another limitation of the present study involves the contribution of asymptomatic infections. The current model was formulated at a time when the contribution of asymptomatic infections was still being debated, with many researchers conjecturing the possibility of a reasonable proportion of new infections attributable to asymptomatic infected individuals. However, the major difficulty was ascertaining the actual contribution from asymptomatic individuals and very limited studies had considered including asymptomatic individuals in their modeling framework. Hence, the non-inclusion of this class in the current model. However, the current model can be further improved by incorporating a class of asymptomatically infected individuals, depending on the availability of more information on this aspect. The results presented in this paper are actionable and hold the potential to inform policy management and decision-making regarding the control of future outbreaks of the COVID-19 pandemic in Zimbabwe and beyond.

## Declaration of competing interest

The authors declare that we do not have any competing interests regarding the production of the above-mentioned manuscript.

## Data availability

Data will be made available on request.

## Acknowledgments

The authors acknowledge, with thanks, the support of their respective departments towards the production of this manuscript.

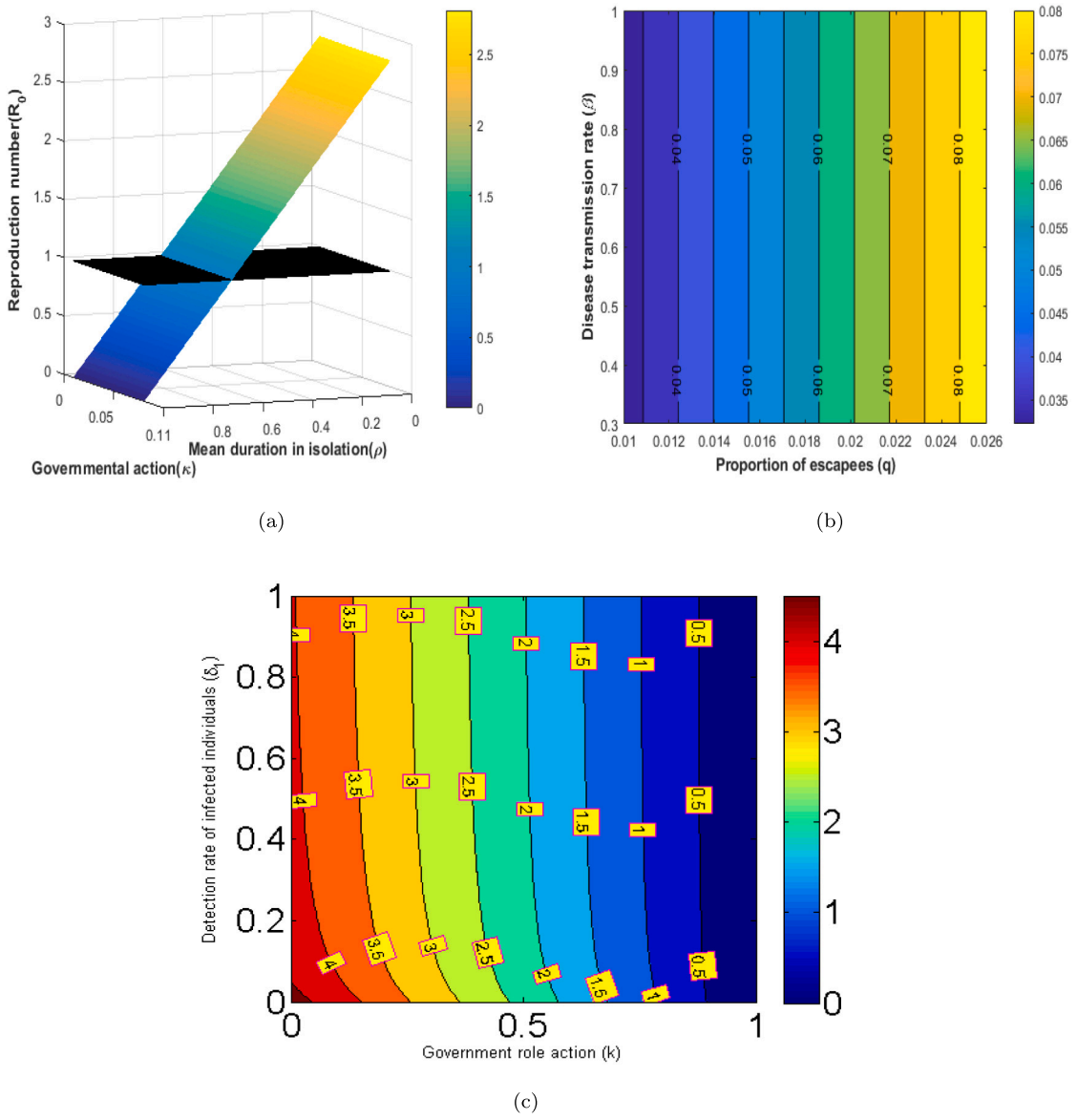


**Fig. 13.** (a) 3D plot of parameters governmental action and mean duration in isolation versus the model basic reproduction number, $\mathcal{R}_0$. (b) Contour plots of the model parameters proportion of escapees ($q$) versus disease transmission rate, $\beta$. (c) Contour plots of the model parameters governmental role action ($\kappa$) versus detection rate of infected individuals, $\delta_1$.

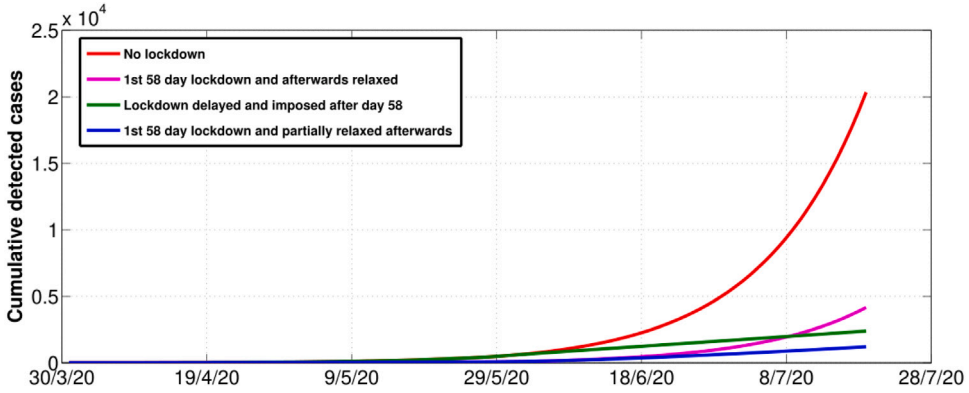


**Fig. 14.** Simulation of cumulative detected cases under different lockdown scenarios.

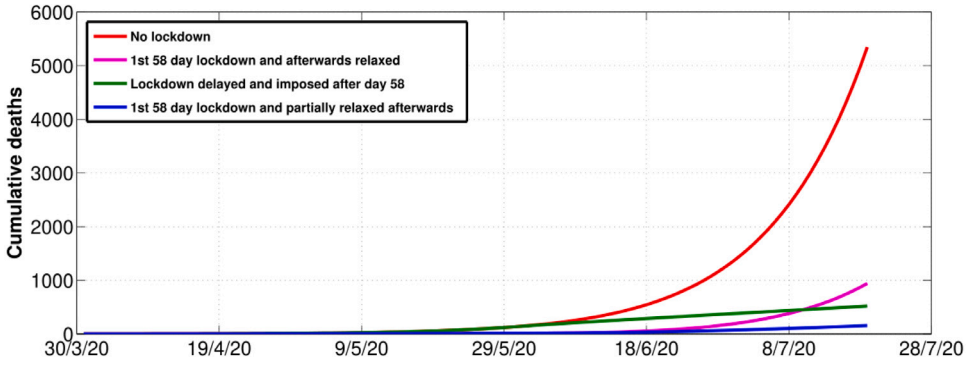


**Fig. 15.** Simulation of cumulative deaths under different lockdown scenarios.

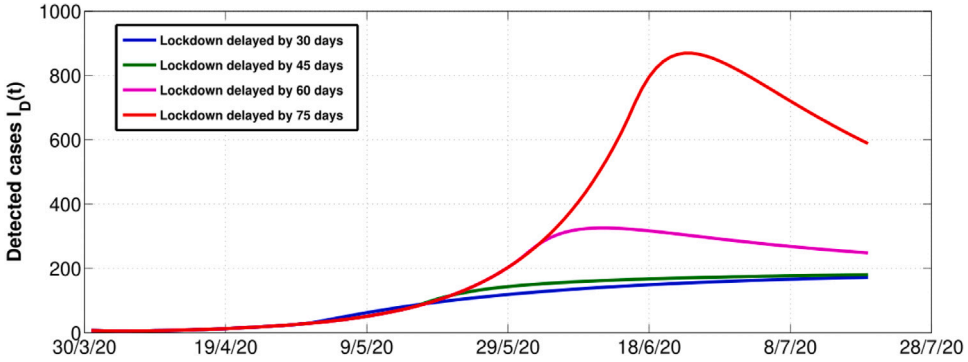


**Fig. 16.** Simulation of daily detected cases for different delays in implementing lockdown measures.

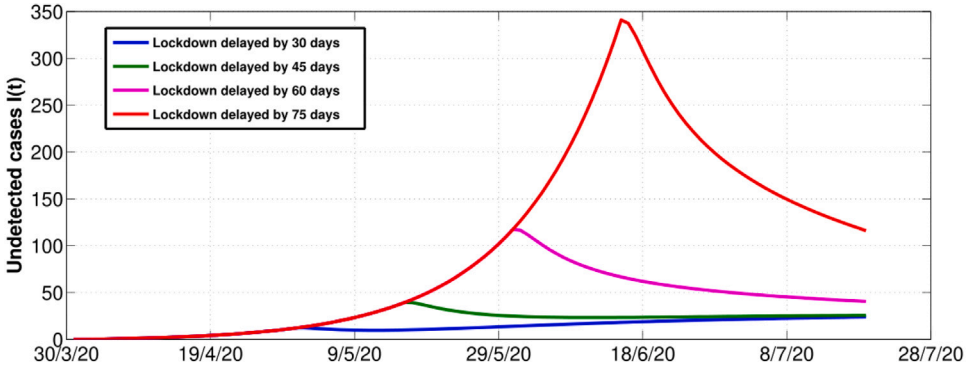


**Fig. 17.** Simulation of daily undetected cases for different delays in implementing lockdown measures.

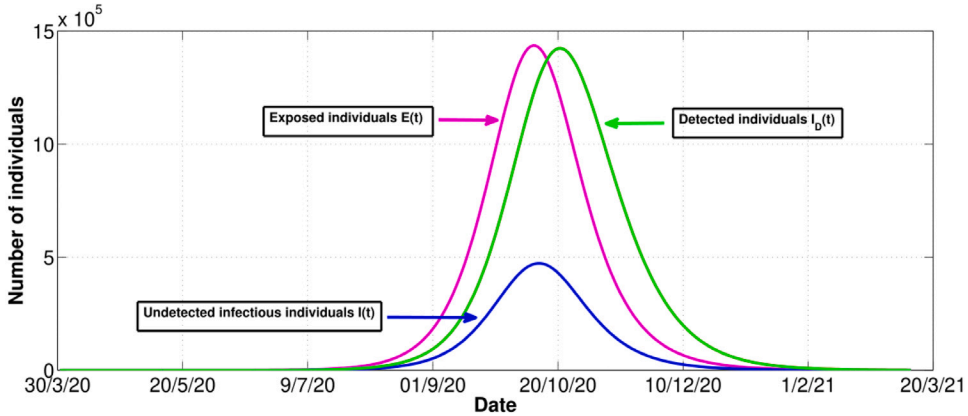


**Fig. 18.** Simulation of projected peak cases of COVID-19 in the presence of escapees.

## References


[1] Coronavirus Update (Live): 13, 141, 440 Cases and 573, 349 Deaths from COVID-19 Virus Pandemic - Worldometer: https://www.worldometers.info/coronavirus/. Accessed 2020-07-14., URL https://www.worldometers.info/coronavirus/, Library Catalog: www.worldometers.info.

[2] South Africa Coronavirus: 287, 796 Cases and 4, 172 Deaths - Worldometer: https://www.worldometers.info/coronavirus/country/south-africa/ Accessed 2020-07-14., URL https://www.worldometers.info/coronavirus/country/south-africa/.

[3] Zimbabwe Coronavirus: https://www.worldometers.info/coronavirus/country/zimbabwe/, Accessed 2020-07-14, URL https://www.worldometers.info/coronavirus/country/zimbabwe/, Library Catalog: www.worldometers.info.

[4] 4 more returnees escape from quarantine | The Herald, URL https://www.herald.co.zw/4-more-returnees-escape-from-quarantine-2/.

[5] S. Mushayabasa, E.T. Ngarakana-Gwasira, J. Mushanyu, On the role of governmental action and individual reaction on COVID-19 dynamics in South Africa: A mathematical modelling study, Inform. Med. Unlocked 20 (2020) 100387.

[6] Y. Tang, S. Wang, Mathematic modeling of COVID-19 in the United States, Emerg. Microb. Infect. 9 (1) (2020) 827–829.

[7] S. Roy, K. Roy Bhattacharya, Spread of COVID-19 in India: A mathematical model, 2020, Available at SSRN 3587212.

[8] S. Gao, P. Binod, C.W. Chukwu, T. Kwofie, S. Safdar, L. Newman, S. Choe, B.K. Datta, W.K. Attipoe, W. Zhang, et al., A mathematical model to assess the impact of testing and isolation compliance on the transmission of COVID-19, Infect. Dis. Modell. 8 (2) (2023) 427–444.

[9] S. Gatyeni, C. Chukwu, F. Chirove, F. Nyabadza, et al., Application of optimal control to the dynamics of COVID-19 disease in South Africa, Sci. Afr. 16 (2022) e01268.

[10] J. Mushanyu, W. Chukwu, F. Nyabadza, G. Muchatibaya, Modelling the potential role of super spreaders on COVID-19 transmission dynamics, Int. J. Math. Modell. Numer. Optim. 12 (2) (2022) 191–209.

[11] S. Wu, Z. Huang, S. Grant-Muller, D. Gu, L. Yang, Modelling the reopen strategy from dynamic zero-COVID in China considering the sequela and reinfection, Sci. Rep. 13 (1) (2023) 7343.

[12] A.K. Srivastav, M. Ghosh, S.R. Bandekar, Modeling of COVID-19 with limited public health resources: a comparative study of three most affected countries, Eur. Phys. J. Plus 136 (2021) 1–26.

[13] E. Acheampong, E. Okyere, S. Iddi, J.H. Bonney, J.K.K. Asamoah, J.A. Wattis, R.L. Gomes, Mathematical modelling of earlier stages of COVID-19 transmission dynamics in ghana, Results Phys. 34 (2022) 105193.

[14] S.R. Bandekar, M. Ghosh, Mathematical modeling of COVID-19 in India and nepal with optimal control and sensitivity analysis, Eur. Phys. J. Plus 136 (2021) 1–25.

[15] C.J. Edholm, B. Levy, L. Spence, F.B. Agusto, F. Chirove, C.W. Chukwu, D. Goldsman, M. Kgosimore, I. Maposa, K.J. White, et al., A vaccination model for COVID-19 in gauteng, South Africa, Infect. Dis. Modell. 7 (3) (2022) 333–345.

[16] C. Chukwu, R. Alqahtani, C. Alfiniyah, F. Herdicho, et al., A pontryagin's maximum principle and optimal control model with cost-effectiveness analysis of the COVID-19 epidemic, Decis. Anal. J. (2023) 100273.

[17] O.J. Peter, N.D. Fahrani, C. Chukwu, et al., A fractional derivative modeling study for measles infection with double dose vaccination, Healthc. Anal. 4 (2023) 100231.

[18] A.K. Saha, S. Saha, C.N. Podder, Effect of awareness, quarantine and vaccination as control strategies on COVID-19 with co-morbidity and re-infection, Infect. Dis. Modell. 7 (4) (2022) 660–689.

[19] S. Khajanchi, K. Sarkar, S. Banerjee, Modeling the dynamics of COVID-19 pandemic with implementation of intervention strategies, Eur. Phys. J. Plus 137 (1) (2022) 129.

[20] J. Mondal, S. Khajanchi, Mathematical modeling and optimal intervention strategies of the COVID-19 outbreak, Nonlinear Dynam. 109 (1) (2022) 177–202.

[21] J.N. Paul, S.S. Mirau, I.S. Mbalawata, et al., Mathematical approach to investigate stress due to control measures to curb covid-19, Comput. Math. Methods Med. 2022 (2022).

[22] M. Rabiu, S.A. Iyaniwura, Assessing the potential impact of immunity waning on the dynamics of COVID-19 in South Africa: an endemic model of COVID-19, Nonlinear Dynam. 109 (1) (2022) 203–223.

[23] R. Kumar Rai, P. Kumar Tiwari, S. Khajanchi, Modeling the influence of vaccination coverage on the dynamics of COVID-19 pandemic with the effect of environmental contamination, Math. Methods Appl. Sci. 46 (12) (2023) 12425–12453.

[24] S. Khajanchi, K. Sarkar, J. Mondal, K.S. Nisar, S.F. Abdelwahab, Mathematical modeling of the COVID-19 pandemic with intervention strategies, Results Phys. 25 (2021) 104285.

[25] P.K. Tiwari, R.K. Rai, S. Khajanchi, R.K. Gupta, A.K. Misra, Dynamics of coronavirus pandemic: effects of community awareness and global information campaigns, Eur. Phys. J. Plus 136 (10) (2021) 994.

[26] F. Nyabadza, F. Chirove, C. Chukwu, M.V. Visaya, Modelling the potential impact of social distancing on the COVID-19 epidemic in South Africa, Comput. Math. Methods Med. 2020 (2020).

[27] B. Ambikapathy, K. Krishnamurthy, Mathematical modelling to assess the impact of lockdown on COVID-19 transmission in India: Model development and validation, JMIR Public Health Surveill. 6 (2) (2020) e19368.

[28] H. Ziauddeen, N. Subramaniam, D. Gurdasani, Modelling the impact of lockdown-easing measures on cumulative COVID-19 cases and deaths in England, BMJ open 11 (9) (2021) e042483.

[29] J.-T. Brethouwer, A. van de Rijt, R. Lindelauf, R. Fokkink, "Stay nearby or get checked": A COVID-19 control strategy, Infect. Dis. Modell. 6 (2021) 36–45.

[30] R.O. Stutt, R. Retkute, M. Bradley, C.A. Gilligan, J. Colvin, A modelling framework to assess the likely effectiveness of facemasks in combination with 'lock-down'in managing the COVID-19 pandemic, Proc. R. Soc. Lond. Ser. A Math. Phys. Eng. Sci. 476 (2238) (2020) 20200376.

[31] K. Prem, Y. Liu, T.W. Russell, A.J. Kucharski, R.M. Eggo, N. Davies, S. Flasche, S. Clifford, C.A. Pearson, J.D. Munday, et al., The effect of control strategies to reduce social mixing on outcomes of the COVID-19 epidemic in wuhan, China: a modelling study, Lancet Public Health (2020).

[32] D. Welle, (www.dw.com), Will mutations soon make the Coronavirus less harmful? | DW | 17.06.2020, URL https://www.dw.com/en/will-mutations-soon-make-the-coronavirus-less-harmful/a-53839943, Library Catalog: www.dw.com.

[33] A.B. Gumel, S. Ruan, T. Day, J. Watmough, F. Brauer, P. van den Driessche, D. Gabrielson, C. Bowman, M.E. Alexander, S. Ardal, et al., Modelling strategies for controlling SARS outbreaks, Proc. R. Soc. B 271 (1554) (2004) 2223–2232.

[34] R.I. Gweryina, C.E. Madubueze, F.S. Kaduna, Mathematical assessment of the role of denial on COVID-19 transmission with non-linear incidence and treatment functions, Sci. Afr. (2021) e00811.

[35] P. van den Driessche, J. Watmough, Reproduction numbers and sub-threshold endemic equilibria for compartmental models of disease transmission, Math. Biosci. 180 (1–2) (2002) 29–48.

[36] Z. Shuai, P. van den Driessche, Global stability of infectious disease models using Lyapunov functions, SIAM J. Appl. Math. 73 (4) (2013) 1513–1532.

[37] J.P. LaSalle, An invariance principle in the theory of stability, 1966.

[38] M. Martcheva, An introduction to mathematical epidemiology, Texts Appl. Math. 61 (2015) 142–143.

[39] Zimbabwe situation report 10 July 2020: https://reliefweb.int/report/zimbabwe/zimbabwe-situation-report-10-july-2020, URL https://reliefweb.int/report/zimbabwe/zimbabwe-situation-report-10-july-2020.

[40] Zimbabwe authorities indefinitely extend COVID-19 lockdown measures May 16 update: https://www.garda.com/crisis24/news-alerts/342951/zimbabwe-authorities-indefinitely-extend-covid-19-lockdown-measures-may-16-update-8., URL https://www.garda.com/crisis24/news-alerts/342951/zimbabwe-authorities-indefinitely-extend-covid-19-lockdown-measures-may-16-update-8.

[41] Zimbabwe extends virus lockdown for indefinite period : https://www.aa.com.tr/en/africa/zimbabwe-extends-virus-lockdown-for-indefinite-period/{1843457}, URL https://www.aa.com.tr/en/africa/zimbabwe-extends-virus-lockdown-for-indefinite-period/1843457.

[42] COVID-19 daily updates: http://www.mohcc.gov.zw/index.php?, URL http://www.mohcc.gov.zw/index.php?option=com_phocadownload&view=category&id=15:covid-19-daily-updates&Itemid=741.

[43] A.A. Balcha, et al., Curve fitting and least square analysis to extrapolate for the case of COVID-19 status in ethiopia, Adv. Infect. Dis. 10 (03) (2020) 143.

[44] A. Assiri, A. McGeer, T.M. Perl, C.S. Price, A.A. Al Rabeeah, D.A. Cummings, Z.N. Alabdullatif, M. Assad, A. Almulhim, H. Makhdoom, et al., Hospital outbreak of middle east respiratory syndrome coronavirus, N. Engl. J. Med. 369 (5) (2013) 407–416.

[45] S. Usaini, A.S. Hassan, S.M. Garba, J.-S. Lubuma, Modeling the transmission dynamics of the middle east respiratory syndrome coronavirus (MERS-CoV) with latent immigrants, J. Interdiscip. Math. 22 (6) (2019) 903–930.

[46] Guidance for discharge and ending isolation in the context of widespread community transmission of COVID-19 – first update:https://www.ecdc.europa.eu/sites/default/files/documents/covid-19-guidance-discharge-and-ending-isolation-first update.pdf. Accessed 2020-07-16, URL https://www.ecdc.europa.eu/sites/default/files/documents/covid-19-guidance-discharge-and-ending-isolation-first%20update.pdf.

[47] P.V. Savi, M.A. Savi, B. Borges, A mathematical description of the dynamics of the coronavirus disease 2019 (COVID-19): a case study of Brazil, 2004.

[48] World Health Organization, Coronavirus disease 2019 (COVID-19) Situation Report, Accessed 09-07-2020, URL https://www.who.int/docs/default-source/coronaviruse/situation-reports/20200402-sitrep-73-covid-19.pdf?sfvrsn=5ae25bc7_4.

[49] S.A. Lauer, K.H. Grantz, Q. Bi, F.K. Jones, Q. Zheng, H.R. Meredith, A.S. Azman, N.G. Reich, J. Lessler, The incubation period of coronavirus disease 2019 (COVID-19) from publicly reported confirmed cases: estimation and application, Ann. Internal Med. 172 (9) (2020) 577–582.

[50] Report of the WHO-China joint mission on Coronavirus disease 2019 (COVID-19), URL https://www.who.int/docs/default-source/coronaviruse/who-china-joint-mission-on-covid-19-final-report.pdf.

[51] B. Ivorra, M.R. Ferrández, M. Vela-Pérez, A. Ramos, Mathematical modeling of the spread of the coronavirus disease 2019 (COVID-19) taking into account the undetected infections. The case of China, Commun. Nonlinear Sci. Numer. Simul. (2020) 105303.

[52] World Health Organization, Coronavirus disease 2019 COVID-19 Situation Report–46, URL https://www.who.int/docs/default-source/coronaviruse/situation-reports/20200306-sitrep-46-covid-19.pdf?sfvrsn=96b04adf_4.

[53] S. Marino, I.B. Hogue, C.J. Ray, D.E. Kirschner, A methodology for performing global uncertainty and sensitivity analysis in systems biology, J. Theoret. Biol. 254 (1) (2008) 178–196.